Microbiology (2012), **158**, 1094–1105 **DOI** 10.1099/mic.0.056119-0

NhaP1 is a $K^+(Na^+)/H^+$ antiporter required for growth and internal pH homeostasis of *Vibrio cholerae* at low extracellular pH

Matthew J. Quinn,[1,2] Craig T. Resch,[3] Jonathan Sun,[1] Erin J. Lind,[2] Pavel Dibrov[3] and Claudia C. Häse[1,2]

[1]Department of Microbiology, Oregon State University, Corvallis, OR 97331, USA

[2]Department of Biomedical Sciences, College of Veterinary Sciences, Oregon State University, Corvallis, OR 97331, USA

[3]Department of Microbiology, University of Manitoba, Winnipeg, Manitoba R3T 2N2, Canada

Correspondence
Claudia C. Häse
claudia.hase@oregonstate.edu
Pavel Dibrov
dibrovp@ms.umanitoba.ca

Received 4 November 2011
Revised 16 December 2011
Accepted 5 January 2012

Vibrio cholerae has adapted to a wide range of salinity, pH and osmotic conditions, enabling it to survive passage through the host and persist in the environment. Among the many proteins responsible for bacterial survival under these diverse conditions, we have identified Vc-NhaP1 as a $K^+(Na^+)/H^+$ antiporter essential for *V. cholerae* growth at low environmental pH. Deletion of the *V. cholerae nhaP1* gene caused growth inhibition when external potassium was either limited (100 mM and below) or in excess (400 mM and above). This growth defect was most apparent at mid-exponential phase, after 4–6 h of culture. Using a pH-sensitive GFP, cytosolic pH was shown to be dependent on K^+ in acidic external conditions in a Vc-NhaP1-dependent manner. When functionally expressed in an antiporterless *Escherichia coli* strain and assayed in everted membrane vesicles, Vc-NhaP1 operated as an electroneutral alkali cation/proton antiporter, exchanging K^+ or Na^+ ions for H^+ within a broad pH range (7.25–9.0). These data establish the putative *V. cholerae* NhaP1 protein as a functional $K^+(Na^+)/H^+$ antiporter of the CPA1 family that is required for bacterial pH homeostasis and growth in an acidic environment.

INTRODUCTION

Vibrio cholerae is a Gram-negative pathogen which causes cholera, a dangerous disease that remains a public health concern (Enserink, 2010). As it transitions between the infectious state and its environmental reservoir, the bacterium encounters a dynamic range of osmotic and pH conditions. During human infection, *V. cholerae* produces a potent enterotoxin, cholera toxin, which promotes accumulation of Na^+ and Cl^- ions in the host intestinal lumen and, in turn, causes rapid osmotic dehydration of host tissue and profuse diarrhoea. In the environment, *V. cholerae* is found in many coastal and estuarine waters, where it is exposed to severe periodic changes in salinity, pH and osmolarity as variable ratios of brackish and fresh water mix at different rates (Miller *et al.*, 1984; Singleton *et al.*, 1982a, b). Thus, both the pathogenic and environmental lifestyles of this organism require that *V. cholerae* can adapt to rapidly shifting osmolarities, ionic strengths and pH values. These lifestyles require that *V. cholerae* possess adequate molecular mechanisms to adapt to such environmental challenges.

Abbreviations: BTP, Bistris propane; CCCP, carbonyl cyanide *m*-chlorophenylhydrazone.

A number of *V. cholerae* proteins have been described that generate, maintain or use a transmembrane gradient of cations such as Na^+ (Häse *et al.*, 2001). These proteins are predicted to help the bacterium survive hypo- and hyperosmolar states in addition to exploiting the Na^+ gradient for solute transport, pH regulation and motility. For example, the NQR complex couples Na^+ export to electron transport, resulting in the generation of a sodium-motive force that can then be used for various types of membrane work (Tokuda & Unemoto, 1981, 1982; Zhou *et al.*, 1999). The *V. cholerae* NhaA antiporter mediates Na^+/H^+ exchange and thus regulates Na^+ homeostasis at pH 8.5, conditions which are not unusual for seawater in areas where *V. cholerae* is endemic (Vimont & Berche, 2000). The NhaD antiporter from *V. cholerae* expressed in *Escherichia coli* subbacterial vesicles was shown to be a specific Na^+/H^+ antiporter most active at pH 8.0 (Dzioba *et al.*, 2002), whereas the *V. cholerae* Mrp complex is an electrogenic cation/proton exchanger of broad specificity, exchanging Na^+, K^+ and Li^+ with maximum activity at pH 9.0–9.5 (Dzioba-Winogrodzki *et al.*, 2009). Several membrane systems exploit the transmembrane Na^+ gradient generated by primary (e.g. NQR) or secondary (e.g. NhaA) sodium pumps to drive nutrient acquisition and motility (see Häse

et al., 2001). The Na^+ ions which consequently accumulate in the bacterial cytoplasm are then again expelled by antiporters or NQR, resulting in internal cation homeostasis within dynamic external environments.

K^+/H^+ antiport activity has also been demonstrated in the *Vibrio* species *V. alginolyticus* (Nakamura *et al.*, 1984; Tokuda *et al.*, 1981), *V. parahaemolyticus* (Radchenko *et al.*, 2006), and recently *V. cholerae* (Resch *et al.*, 2010). In *V. alginolyticus*, such activity has been shown to participate in regulation of cytoplasmic pH in acidic media (Nakamura *et al.*, 1984, 1992). Although a K^+/H^+ antiporter was implicated in cytoplasmic pH maintenance in *V. alginolyticus*, the ion transporter responsible has not been identified. Many *Vibrio* species have three paralogues of NhaP (Table 1), a family of bacterial cation/proton antiporters identified by amino acid homology that generally pump Na^+ or K^+ (Resch *et al.*, 2010). The NhaP2 homologue from *V. cholerae* was recently shown to have K^+/H^+ antiport activity in the parent as well as *E. coli* strains, showing also a unique response to Li^+ and strong *in vitro* activity (Resch *et al.*, 2010). The *V. cholerae* NhaP2 antiporter was found to be a K^+/H^+ antiporter most active at low pH (6.0) which is indispensable for the growth of *V. cholerae* at extracellular potassium concentrations of 400 mM or greater in acidic media, removing excess of internal K^+ from the cytoplasm at the expense of ΔpH (Resch *et al.*, 2010). The NhaP2 protein from *V. parahaemolyticus* was similarly shown to be involved in K^+/H^+ antiport at high concentrations of potassium when expressed ectopically in *E. coli* (Radchenko *et al.*, 2006). As the NhaP2 antiporter is only one of three putative NhaP paralogues in *V. cholerae* identified by sequence similarity, we intend to also characterize the role of the other putative NhaP proteins, beginning with Vc-NhaP1, to assess their relative contribution to the overall cytoplasmic ion homeostasis.

Here, we report the detailed characterization of the putative *V. cholerae* NhaP1 protein, encoded by VC0389 (NP#230338.1). We performed growth analysis of a defined in-frame *V. cholerae nhaP1* deletion mutant and compared the ability of the parental strain and its isogenic mutant strain to regulate cytoplasmic pH. We also assayed key biochemical features of the Vc-NhaP1 protein expressed in an *E. coli* strain lacking three major cation/proton antiporters. To our knowledge, the results presented represent the first detailed physiological and biochemical analyses of an NhaP1-type antiporter.

METHODS

Bacterial strains and culture conditions. The Na^+/H^+ antiporter-deficient strain of *E. coli* TO114 [F^- IN(*rrnD–rrnE*) *nhaA*::Km^R *nhaB*::Em^R *chaA*::Cm^R] was kindly provided by H. Kobayashi (Faculty of Pharmaceutical Sciences, Chiba University, Chiba, Japan) (Radchenko *et al.*, 2006). For routine cloning and plasmid construction, *E. coli* DH5α (*supE44 hsdR17 recA1 endA1, gyrA96 thi-1 relA1*) (US Biochemical Corp.) or TOP10 [F^- *mcr*A Δ(*mrr–hsdRMS-mcrBC*) *ϕ*80*lacZ*ΔM15 Δ*lacX74 rec*A*1 araD139* Δ(*ara leu*)7697 *galU galK rpsL* (Str^R) *endA1 nupG*] (Invitrogen) was used as the host. *V. cholerae* strain O395N1 was used in this study (Mekalanos *et al.*, 1983); this is a

Table 1. Homology of monovalent cation/proton antiporter-2 (CPA2) family antiporters (HMM PF00999) of *Vibrio* species predicted from bioinformatic analyses

Locus: gene (and name, where available). Antiporter type: most similar *V. cholerae* homologue (HMM match: match value to the HMM CPA2 motif). *V. cholerae* identity: amino acid identity to the closest *V. cholerae* CPA2 family paralogue (NA, not applicable).

Locus	Antiporter type	*V. cholerae* identity	*Vibrio* species
VC0389 (Vc-NhaP1)	(CPA2) family antiporter (HMM PF00999, HMM match 2.6e–70)	NA	
VC2703 (Vc-NhaP2)	(CPA2) family antiporter (HMM PF00999, HMM match 7.2e–72)	NA	*V. cholerae*
VC0689 (Vc-NhaP3)	(CPA2) family antiporter (HMM PF00999, HMM match 1.3e–26)	NA	
VMD_33930	VC-nhaP1-type antiporter	423/443 (95 %)	
VMD_05140	VC-nhaP2-type antiporter	557/571 (98 %)	*V. mimicus*
VMD_04400	VC-nhaP3-type antiporter	581/599 (97 %)	
VV2961	VC-nhaP1-type antiporter	385/431 (89 %)	*V. vulnificus*
VV0696	VC-nhaP3-type antiporter	444/598 (74 %)	
V12G01_14609	VC-nhaP1-type antiporter	365/418 (87 %)	
V12G01_00925	VC-nhaP2-type antiporter	481/578 (83 %	*V. alginolyticus*
V12G01_02860	VC-nhaP3-type antiporter	421/589 (71 %)	
V12B01_10612	VC-nhaP1-type antiporter	381/426 (89 %)	*V. splendidus*
V12B01_01622 (CvrA)	VC-nhaP2-type antiporter	418/582 (72 %)	
VP2718	VC-nhaP1-type antiporter	387/443 (87 %)	
VP2867	VC-nhaP2-type antiporter	485/571 (85 %)	*V. parahaemolyticus*
VPA0277	VC-nhaP3-type antiporter	421/587 (72 %)	

classical Ogawa strain with a deletion in the *ctxA* gene (O1 classical biotype; Sm^R, Δ*ctxA*1). If not otherwise indicated, TO114 cells were grown aerobically at 37 °C in LBK medium [modified L broth in which NaCl was replaced with KCl (Padan *et al.*, 1989)] supplemented with 100 μg ampicillin ml^{-1}, 30 μg kanamycin ml^{-1}, 34 μg chloramphenicol ml^{-1}, 100 μg erythromycin ml^{-1} and 0.05 % (w/v) arabinose. *V. cholerae* cells were grown aerobically at 37 °C in LB supplemented with 100 μg streptomycin ml^{-1}, 100 μg ampicillin ml^{-1} and 0.02 % (w/v) arabinose, unless otherwise indicated. Cytoplasmic pH experiments were conducted in K100 medium, a minimal salts medium with K^+, and K0 medium, in which K^+ salts were replaced with Na^+ salts (Epstein & Kim, 1971); cytoplasmic pH was measured in pH medium [150 mM choline chloride and 60 mM Bistris propane (BTP) adjusted to pH 6.0, 6.5 or 7.2].

Cloning and expression of Vc-NhaP1. Sequence data for *V. cholerae* were obtained from the Institute for Genomic Research (http://www.jcvi.org). Cloning was performed as described before (Resch *et al.*, 2010). The putative *Vc-nhaP1* ORF was amplified by high-fidelity PCR, using chromosomal DNA of *V. cholerae* O395N1 as a template and directly cloned into the pBAD-TOPO vector (Invitrogen) under the arabinose-induced promoter (P_{BAD}), yielding pVc-NhaP1. The following primers were used for cloning: forward primer VcNhaP1expF, 5′-GAGGAATAATAAATGTCCGTCTACTACACTTG-3′; and reverse primer VcNhaP1expR, 5′-TTAGTGTTGTTGTTCTTGCTG-3′. The forward primer was designed to achieve expression of the native enzyme without addition of the N-terminal leader sequence usually introduced by this vector. The primer contains an in-frame stop codon and a translation reinitiation sequence, which consists of a ribosome-binding site and the first ATG of the protein. In the reverse primer, the native stop codon of *Vc-nhaP1* was maintained. Using these primers, the *nhaP1* ORF was amplified by PCR as described previously. Briefly, 1 unit of Platinum PCR Supermix High Fidelity DNA polymerase (Invitrogen) was used to amplify the approximately 1.3 kb fragment corresponding to *Vc-nhaP1*, a portion of which was run on a gel to confirm the amplicon size. The remainder of the PCR mixture was purified using the QIAquick PCR Purification kit (Qiagen), and was then introduced into the pBAD-TOPO vector using the manufacturer's protocol (Invitrogen). Transformants were screened by PCR for the correct orientation by using a forward primer for the plasmid (pBAD Forward) and the 3′ expression primer for the gene. Plasmid extractions were performed using the QIAprep Spin Miniprep kit (Qiagen) and the fidelity of the PCR was confirmed by DNA sequencing at the Oregon State University Center for Genome Research and Biocomputing core lab facility. This pVc-NhaP1 construct was then introduced into *E. coli* TO114 by chemical transformation and into *V. cholerae* O395N1Δ*nhaP1* (see below) by electroporation as described previously (Hamashima *et al.*, 1995).

Chromosomal deletion of the *Vc-nhaP1* gene. Chromosomal deletion of the *Vc-nhaP1* gene was conducted by homologous recombination. The defined mutant construct was made using overlap extension PCR (Ho *et al.*, 1989). A 1 kb fragment upstream of the start codon was amplified from genomic DNA by PCR using the following primer pair: 1, 5′-GGGGGGGATCCGCATTCTGAAATGCGTGAAAG-3′; and 2, 5′-GACTGACTGACTGACTGACTGACTCATTCTCTTCTCAGTGTGTGTAACAATTTG-3′. A 1 kb fragment downstream of the stop codon was amplified from genomic DNA by PCR using the following primer pair: 3, 5′-AGTCAGTCAGTCAGTCAGTCAGTCTAATCTCCGTTGTTTAATCGACAAAC-3′; and 4, 5′-GGGGGGAGCTCAAGTTCGGAATTGATAAGCGC-3′. The DNA products of these two PCRs are able to anneal together due to complementary sequences engineered into primers 2 and 3 and were used as a template for a third PCR using primers 1 and 4, resulting in a 2 kb PCR product encompassing 1 kb upstream of the start codon and 1 kb downstream of the stop codon with the gene itself removed. This PCR product was cloned into suicide vector pWM91 (Metcalf *et al.*, 1996) by restriction sites engineered into primers 1 and 4, and the mutant allele was introduced into the chromosome of *V. cholerae* O395N1 following conjugation with the *E. coli* strain hosting the vector. Using sucrose selection (Metcalf *et al.*, 1996), the in-frame deletion of the ORF was introduced into the chromosome of *V. cholerae* strain O395N1. This mutant strain (O395N1Δ*nhaP1*) along with its isogenic parent (O395N1) and O395N1Δ*nhaP1*/pVc-NhaP1 overexpressing the *V. cholerae nhaP1* gene *in trans* and O395N1/pBAD24 were used to assess the function of Vc-NhaP1.

Analysis of growth phenotypes. For growth analysis of *V. cholerae* strains, LBB medium (non-cationic L broth) was supplemented with antibiotics, arabinose and varying concentrations of NaCl, KCl, LiCl, $MgCl_2$, $CaCl_2$, $CuCl_2$, $FeCl_3$ or L-proline. The initial pH of the media was adjusted with HCl to 6.0, 7.2 or 8.5 and buffered by the addition of 60 mM BTP. Cells were inoculated into 200 μl liquid medium in 96-deep-well plates (Whatman) at an initial OD_{600} of 0.05 and grown at 37 °C for 18 h with vigorous aeration. Growth was then measured as OD_{600} by scanning the plates on a Bio-Rad iMark microplate absorbance reader. All experiments were repeated at least three times in triplicate.

Measurement of cytoplasmic pH *in vivo*. Cells of O395N1 and O395N1Δ*nhaP1* were transformed with pMMB1311 (encoding GFPmut3b, a pH-sensitive GFP) (Kitko *et al.*, 2009), yielding strains MJQ0121 and MJQ0122, respectively. Potassium-depleted cells for the pH recovery experiments were obtained essentially as described by Kroll & Booth (1981, 1983). The strains were cultivated overnight at 37 °C in K100 medium (Epstein & Kim, 1971), containing 46 mM K_2HPO_4, 23 mM KH_2PO_4, 8 mM $(NH_4)_2SO_4$, 400 μM $MgSO_4$, 6 μM $FeSO_4$, 1 mM sodium citrate, 1 mg thiamine l^{-1}, 2 g glucose l^{-1}, and supplemented with 100 μg streptomycin ml^{-1} and 100 μg ampicillin ml^{-1}. Cells were pelleted and resuspended to OD_{600} in K0 medium (Epstein & Kim, 1971), in which all potassium salts were substituted by sodium ones. Cells were allowed to grow in K0 medium to OD_{600} 1.0, then placed on ice, pelleted at 2200 r.p.m. at 4 °C for 5 min and resuspended at OD_{600} 0.4 in the pH assay buffer, containing 50 mM choline chloride and 60 mM BTP (pH 6.0). K^+-depleted cells were dispensed in 200 μl aliquots in a 96-well plate, and a baseline reading was taken using a Tecan plate reader (excitation/emission at 480 nm/525 nm) at 37 °C. Glucose (final concentration 1 mM) was added at $t=0$ to energize the cells. After 10 min, KCl was added to experimental wells (final concentration 0–100 mM) and 20 mM benzoate was added to calibration wells to collapse ΔpH, thus equalizing internal pH to external pH, to correlate emission values to internal pH. Data were collected for a further 10 min. All measurements were performed in triplicate in each of three independent experiments. Errors are reported as SD or SEM as indicated in the figure legends; where necessary significance of the results was assessed by Student's *t*-test. For the comparison of steady-state internal pH values, the potassium-, sodium- or choline-loaded cells were prepared using the method of cation replacement advanced by Unemoto and colleagues (Nakamura *et al.*, 1982). Briefly, mid-exponential-phase cultures were pelleted, resuspended in 0.4 M chloride salt of a desired cation containing 50 mM diethanolamine hydrochloride at pH 8.5, and incubated at room temperature for 10 min. Then cells were pelleted by centrifugation, and the treatment was repeated. After that, cells were pelleted again, washed twice and resuspended in 0.4 M chloride salt of a desired cation with 50 mM BTP/HCl (pH 6.0). Prepared cation-loaded cells were assayed immediately. Steady-state internal pH levels were recorded as described above for 10 min.

Isolation of membrane vesicles for assay of antiporter activity. Antiporter activity was measured in inside-out membrane vesicles isolated from the Δ*nhaA* Δ*nhaB* Δ*chaA* strain of *E. coli* TO114

transformed with pVc-NhaP1 or pBAD24. These transformants were grown in LBK medium containing 100 mg ampicillin ml^{-1}, 30 mg kanamycin ml^{-1}, 34 mg chloramphenicol ml^{-1}, 100 mg erythromycin ml^{-1} and 0.05 % arabinose. Cells were harvested at an OD_{600} of 1.0–1.2, washed three times in buffer containing 140 mM choline chloride, 10 % (w/v) glycerol and 20 mM Tris/HCl, pH 7.5, and then lysed using a French press, essentially as described previously (Resch *et al.*, 2010). The unbroken cells were pelleted, the supernatants were ultracentrifuged at 184 000 ***g*** for 90 min at 4 °C, and isolated vesicles were resuspended in the same buffer. For $\Delta\psi$ measurements, vesicles were isolated in the above buffer, but choline chloride was replaced with 280 mM sorbitol.

Measurement of transmembrane ΔpH. For ΔpH measurements, aliquots of vesicles containing approximately 200 mg total protein were added to 2 ml buffer containing 140 mM choline chloride, 5 mM $MgCl_2$, 10 % (w/v) glycerol, 4 mM acridine orange and 50 mM BTP/HCl adjusted to the indicated pH. Measurements of K^+/H^+, Na^+/H^+ and Li^+/H^+ antiporter activities were performed by using the acridine orange fluorescence dequenching assay (Dzioba *et al.*, 2002; Dzioba-Winogrodzki *et al.*, 2009; Resch *et al.*, 2010). Briefly, respiration-dependent ΔpH was generated by the addition of 20 mM Tris/D-lactate and the resulting quenching of acridine orange fluorescence was monitored in a Shimadzu RF-1501 spectrofluorophotometer (excitation at 492 nm and emission at 528 nm). The detected antiport activities were expressed as percentage restoration of lactate-induced fluorescence quenching in response to the addition of 10 mM NaCl, LiCl or KCl at the indicated concentrations. Each experiment was carried out in duplicate from separate isolations of membrane vesicles. The background activity measured in 'empty' vesicles at every pH tested in separate control experiments was subtracted from the levels obtained in Vc-NhaP1-containing vesicles to yield the data shown.

Measurement of transmembrane $\Delta\psi$. Inside-out membrane vesicles (Resch *et al.*, 2010) were isolated from TO114 cells transformed with pVc-NhaP1 or pBAD24 and assayed for $\Delta\psi$ in chloride-free, potassium-free buffer at pH 7.5. Vesicles were mixed with 20 mM diethanolamine for 5 min prior to the addition of 8 mM of the $\Delta\psi$-sensitive dye Oxonol V. Excitation and emission were measured at 595 nm and at 630 nm, respectively.

Materials. All chemicals were purchased from Sigma-Aldrich or Fisher Scientific. Restriction endonucleases and DNA-modifying enzymes were purchased from Invitrogen, MBI Fermentas or New England Biolabs.

RESULTS

Distribution of *nhaP* genes in various *Vibrio* species

In silico analyses revealed that, of the several putative antiporters encoded in the *V. cholerae* genome, three (Vc-NhaP1, Vc-NhaP2 and Vc-NhaP3) are paralogues of each other (Table 1; also see Dzioba-Winogrodzki *et al.*, 2009). These proteins have homologues in other *Vibrio* species as well, and three other *Vibrio* species (*V. parahaemolyticus*, *V. alginolyticus* and *V. mimicus*) encode homologues of all three NhaP paralogues (Table 1). Additionally, NhaP1 is at least 85 % identical to genes in the following sequenced *Vibrio* genomes: *V. cholerae* (2740-80, V52, TM 11079-80, TMA21, RC 385, V51, 623-29, LMA-3894-4, MZO-2, RC 27, CT 5369-93), *V. mimicus* (VM573, MB 451, VM603, VM223), *Vibrio* sp. (RC 586, AND4, Ex25, RC 341, MED222), *V. harveyi* (1DA3, HY01, ATC BAA 1116), *V. vulnificus* (YJ016, CMCP6, MO6-24/O), *V. furnisii* (NCTC 11218), *V. parahaemolyticus* (AQ 3810, RIMID 2210633, K5030, AN-5030, Peru-466, AQ4037), *V. metschnikovii* (CIP 69.14), *V. alginolyticus* (40B), *V. orientalis* (CIP 102891), *V. brasiliensis* (LMG 20546), *V. coralyticus* (ATCC BAA-450), *V. splendidus* (12B01, LGP 32), *V. harveyi* (ATCC BAA-1116), *V. fischeri* (ES 114) and *V. sinaloensis* (DSM 21326). These data show that the *nhaP1* genes are widely conserved among different *Vibrio* species.

Growth properties of the *V. cholerae* Δ*nhaP1* mutant

Deletion of *Vc-nhaP2* leads to a growth deficiency phenotype specifically in media containing 400–500 mM K^+ at pH 6.0 (Resch *et al.*, 2010). For comparison, we measured the effect of pH and K^+ on growth yield in the *V. cholerae* Δ*nhaP1* mutant. After 18 h of aerobic growth, O395N1Δ*nhaP1*, unlike the parent strain, showed markedly lowered growth yield in the media supplemented with K^+ at pH 6.0, with the most severe growth deficiencies observed at 0–100 mM and 400–600 mM added K^+ (Fig. 1a). Complementation *in trans* with the *V. cholerae nhaP1* gene in the arabinose-inducible pBAD system restored the growth phenotype of the parent strain almost completely (Fig. 1a), and the level to which complementation restored the growth phenotype increased as the arabinose concentration was increased (data not shown). No difference in growth was observed between the parent and O395N1Δ*nhaP1* growing in K^+ media at pH 7.2 or 8.5 (Fig. 1b, c). When these experiments were performed with Na^+ or Li^+ added instead of K^+, no growth defects were found in O395N1Δ*nhaP1* at high concentrations of these cations (Fig. 1d–i). It is of note that the growth defect related to the deletion of *nhaP1* persisted in acidic medium at low concentrations of added Na^+ (Fig. 1d). These experiments demonstrate that deletion of *Vc-nhaP1* leads to an inhibited growth phenotype in acidic media (pH 6.0) in two situations: (i) low concentrations of alkali cations or (ii) in the presence of high concentrations of K^+. Standard osmolytes, sucrose (up to 500 mM) and proline (up to 50 mM), were also assayed as possible substitutions for alkali cations. While proline did not affect the growth of the O395N1Δ*nhaP1* mutant at any concentration used, sucrose improved it to some extent, elevating the growth yield for 18 h from OD_{600} 0.4 in the original LBB medium to approximately 0.85 in the same medium supplemented with 300 mM sucrose. It therefore never reached the growth yields typical for the wild-type (of approx. 1.3–1.4; see Fig. 1a). At concentrations exceeding 400 mM, sucrose reduced the growth yield. Thus, the inhibited growth of O395N1Δ*nhaP1* at low ionic strength may be attributed to impaired osmoregulation, but only partially.

To further characterize the growth deficiency revealed in O395N1Δ*nhaP1* growing at pH 6.0 for 18 h (Fig. 1a, d),

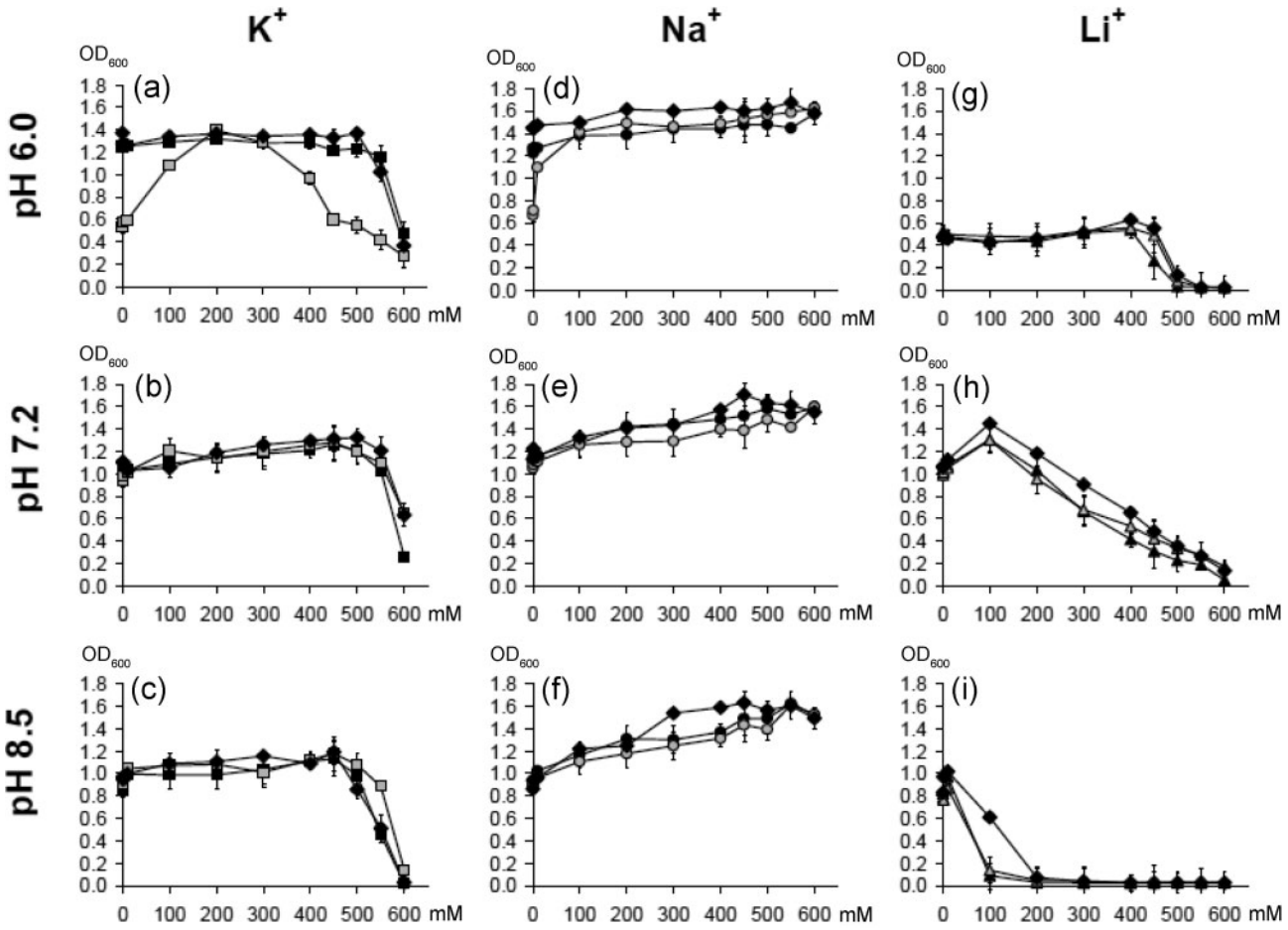

Fig. 1. Growth deficiency in *V. cholerae* Δ*nhaP1*. Growth yields of O395N1/pBAD24 (black diamonds), O395N1Δ*nhaP1*/pVc-NhaP1 (black symbols: squares, KCl; circles, NaCl; triangles, LiCl), and O395N1Δ*nhaP1*/pBAD24 (grey symbols: squares, KCl; circles, NaCl; triangles, LiCl) were determined in LB-based media supplemented with selected cations. OD_{600} values (*y*-axes) of *V. cholerae* cultures were measured after 18 h of aerobic growth in the presence of 0–600 mM (*x*-axes) of either KCl (a–c), NaCl (d–f) or LiCl (g–i). All media were buffered to the indicated pH with 60 mM BTP. Plasmid gene expression was induced by addition of 0.02 % arabinose. Plotted are the means ± SEM of three separate experiments, each performed in triplicate.

dynamics of growth was monitored by taking OD_{600} readings every 60 min (Fig. 2). Interestingly, at 100–400 mM K^+ (Fig. 2b–e) growth of O395N1Δ*nhaP1* was clearly triphasic, whereas O395N1 and O395N1Δ*nhaP1*/pVc-NhaP1 exhibited biphasic growth phenotypes only at 500 mM KCl (Fig. 2f). When the bacteria were grown over a range of NaCl concentrations, no apparent differences were noted in the O395N1Δ*nhaP1* strain compared to O395N1 (Fig. 2i–n). However, a reduced fitness of O395N1Δ*nhaP1* compared to O395N1 or O395N1Δ*nhaP1*/pVc-NhaP1 was noted in the absence of added NaCl (Fig. 2h), as expected.

Cytoplasmic pH homeostasis in the *V. cholerae* Δ*nhaP1* mutant strain

In an attempt to assess the physiological function of Vc-NhaP1 at the biochemical level, we investigated the possible effect of this protein on homeostasis of cytoplasmic pH. First, the ability to recover cytoplasmic pH values was measured in K^+-depleted bacteria by using a pH-sensitive GFP maintained on the pMMB1311 plasmid, which has been used before in *E. coli* (Kitko *et al.*, 2010) and *Bacillus subtilis* (Kitko *et al.*, 2009). After a baseline reading, KCl or NaCl was added to final concentrations of 0 mM, 1 mM (KCl), 10 mM or 100 mM (NaCl), and readings were taken every 2 min for a further 10 min. Relative optical density values were calibrated to pH readings with a standard curve for each experiment (data not shown). At external pH 6.0, K^+-depleted cells of both O395N1 and O395N1Δ*nhaP1* were unable to build up and maintain the pH gradient across the membrane in the choline chloride medium even in the presence of glucose: internal pH was stable at 6.0 for at least 10 min (Fig. 3a). The addition of 10 mM KCl swiftly raised the cytoplasmic

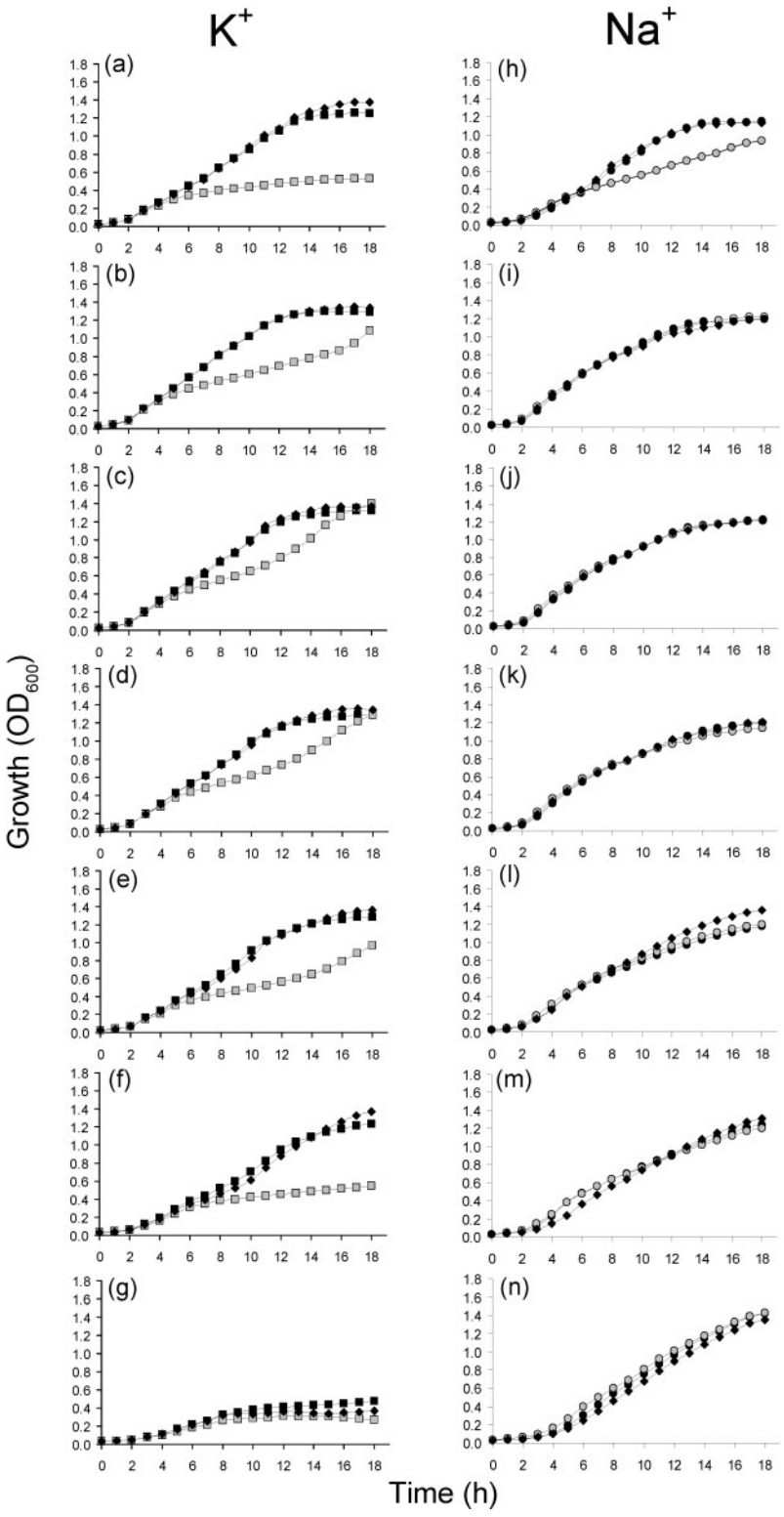

Fig. 2. Growth dynamics of Δ*nhaP1* at different $[K^+]$ and $[Na^+]$. Growth of *V. cholerae* strains was measured every hour as OD at 600 nm in LB-based media supplemented with 0, 100, 200, 300, 400, 500 or 600 mM KCl (a–g, respectively) or the same concentrations of NaCl (h–n, respectively) and buffered with 60 mM BTP at pH 6.0. Gene expression was induced by the addition of 0.02 % arabinose to all media. Growth of O395N1/pBAD24 (black diamonds), O395N1Δ*nhaP1*/pBAD24 (grey symbols: squares, KCl, panels a–g; circles, NaCl, panels h–n), and O395N1Δ*nhaP1*/pVc-*NhaP1* (black symbols: squares, KCl, panels a–g; circles, NaCl, panels h–n) is shown. Plotted are the means of three separate experiments, each performed in triplicate.

pH in cells of O395N1 and O395N1Δ*nhaP1* after approximately 3 min, while up to 100 mM NaCl did not raise the cytoplasmic pH significantly even after 10 min (Fig. 3b). Noticeably, the pH response to added KCl in O395N1Δ*nhaP1* was significantly less pronounced than that in O395N1 (Fig. 3a). In a parallel series of experiments, cells were loaded with different cations as described in Methods, and the steady-state internal pH levels were recorded for 10 min after addition of glucose at external pH 6.0. As Fig. 3(c) shows, the pH homeostasis

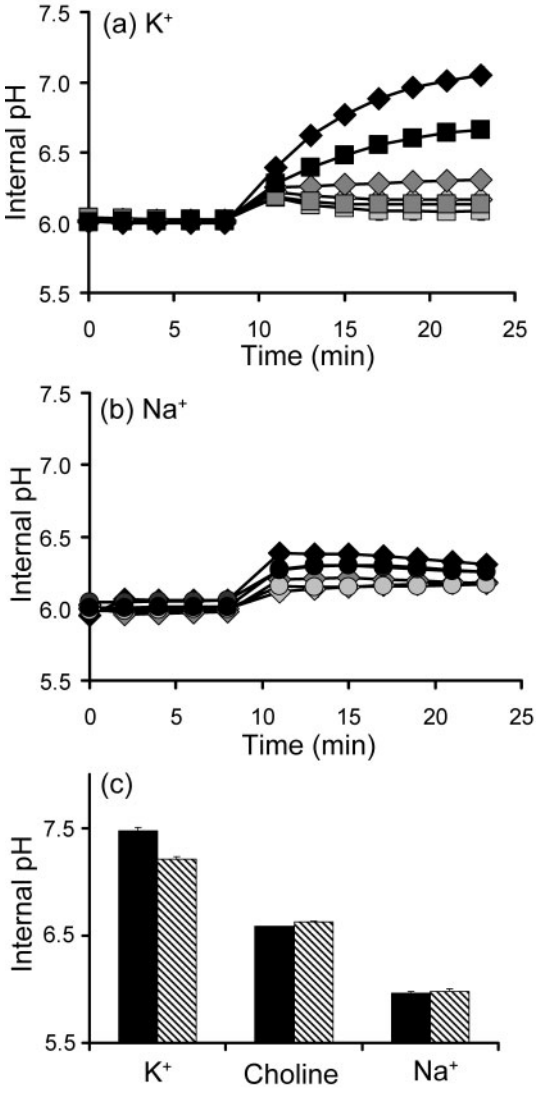

Fig. 3. Vc-NhaP1 as a K^+/H^+ antiporter contributes to the cytoplasmic pH homeostasis in acidic media. (a, b) Internal pH was measured using pGFPmut3b in K^+-depleted cells of O395N1 (diamonds) and O395N1Δ*nhaP1* (squares for K^+ and circles for Na^+) in response to K^+ (a) added at a final concentration of 0 mM (light grey), 1 mM (dark grey) or 10 mM (black), or in response to Na^+ (b) at a final concentration of 0 mM (light grey), 10 mM (dark grey) or 100 mM (black); cations were added at $t=10$ min. (c) Steady-state levels of internal pH in cells of O395N1 (black bars) and O395N1Δ*nhaP1* (hatched bars) loaded with K^+, Na^+ or choline. The pH of the experimental buffer was 6.0 in all cases; 1 mM glucose was added to energize the cells. Plotted are the means ± SEM of three separate experiments over a 10 min period, each performed in triplicate. See the text for further details.

was totally lost in the Na^+-loaded cells of both O395N1 and O395N1Δ*nhaP1*, while the K^+-loaded cells demonstrated internal pH values much closer to the physiological ones. As could be expected from data shown in Fig. 3(a), elimination of functional Vc-NhaP1 resulted in somewhat lower intracellular pH (7.1 vs approx. 7.5 in the wild-type).

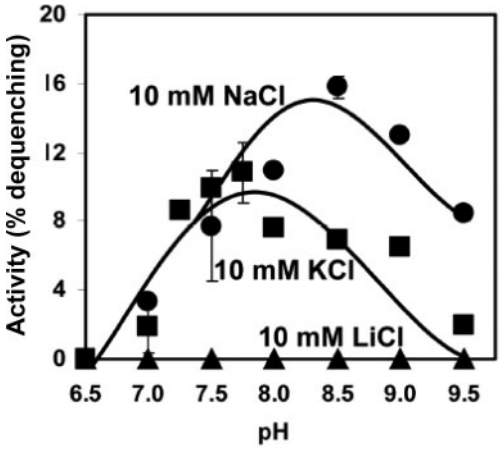

Fig. 4. Cation specificity and pH profiles of Vc-NhaP1 activity. The antiporter was functionally expressed in *E. coli* TO114 and assayed for cation/H^+ antiport in inside-out membrane vesicles prepared as described in Methods. NaCl (circles), KCl (squares) or LiCl (triangles), each at 10 mM, were used to assess the Vc-NhaP1 activity. Antiport activity is expressed as percentage dequenching of acridine orange. For each probe cation and specified pH, the background activity was measured in 'empty' TO114/pBAD24 vesicles and subtracted from the activity measured in Vc-NhaP1 vesicles to yield the data plotted here. In all cases, this background activity did not exceed 10% of dequenching. All measurements were done in triplicate; means ± SD are plotted.

When cells of O395N1 and O395N1Δ*nhaP1* were loaded with choline chloride, they lost pH homeostasis irrespective of the presence of Vc-NhaP1 (data not shown).

Ion specificity and pH profile of Vc-NhaP1 activity

To directly measure antiport activity, we expressed Vc-NhaP1 in cells of the antiport-deficient (Δ*nhaA* Δ*nhaB* Δ*chaA*) *E. coli* strain TO114. Inside-out membrane vesicles from TO114/pVc-NhaP1 and 'empty' TO114/pBAD24 cells were analysed for cation/H^+ antiport activities by the standard acridine orange fluorescence dequenching technique and expressed as percentage restoration of lactate-induced fluorescence quenching. The pH of the assay buffer in this system represents cytosolic pH. When assayed in inside-out membrane vesicles by the addition of 10 mM of KCl, Vc-NhaP1 demonstrated modest but measurable activity in the cytosolic pH range 7.0–9.5 with a relatively broad optimum at cytosolic pH 7.25–8.0 (Fig. 4, squares). When assayed with 10 mM NaCl, Vc-NhaP1 showed a somewhat higher activity from cytosolic pH 7.0 up to the apparently optimal pH of 8.5, with approximately 15% of dequenching (Fig. 4, circles). No activity was detected at or below pH 6.5 with any of the probed cations. Like Vc-NhaP2, Vc-NhaP1 did not show any Li^+/H^+ antiport activity at any of the tested pH values (Fig. 4, triangles). Neither Mg^{2+} nor Ca^{2+} was found to be a substrate of Vc-NhaP1 (data not

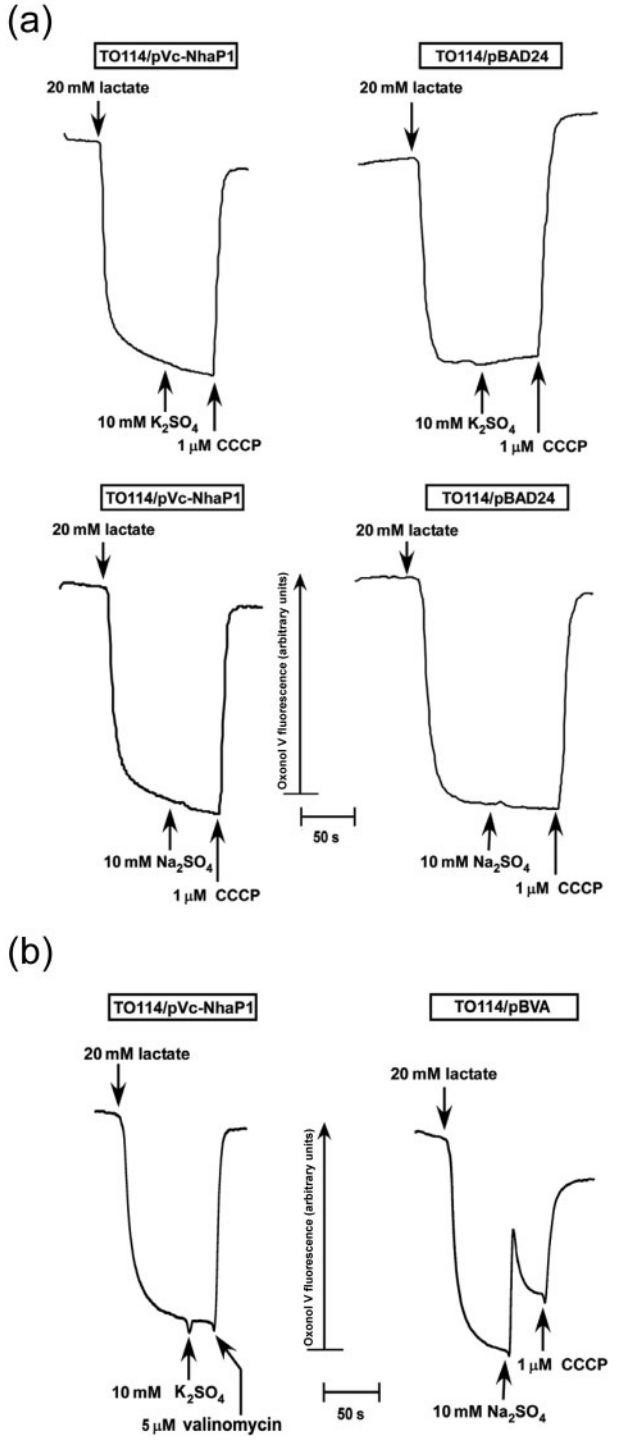

Fig. 5. Probing the electrogenicity of Vc-NhaP1. Inside-out membrane vesicles were isolated from TO114 cells transformed with pVc-NhaP1 or pBAD24 and $\Delta\psi$ was assayed at pH 7.5 in sorbitol-based medium containing no K^+ or Cl^- (a). Vesicles were mixed with 20 mM diethanolamine for 5 min prior to the addition of Oxonol V and respiration-dependent formation of the transmembrane electrical gradient was initiated by the addition of 20 mM Tris/D-lactate. After steady-state $\Delta\psi$ was reached, cation/H^+ antiporter activity was initiated by the addition of 10 mM K_2SO_4 (a, upper traces; b, left trace) or 10 mM Na_2SO_4 (a, lower traces). Control addition of the protonophore CCCP (a) or valinomycin in the presence of K^+ (b, left trace) at the end of each trace completely dissipated respiratory $\Delta\psi$. As a positive control, the TO114/pBVA vesicles expressing the electrogenic Vc-NhaA (Resch *et al.*, 2010) were also assayed under the same conditions (b, right trace). Immediate partial depolarization upon addition of Na^+ in this case indicates the electrogenic character of the ion exchange catalysed by Vc-NhaA.

shown). These *in vitro* kinetic data obtained in the inside-out membrane vesicle model suggest that Vc-NhaP1 is a cation/proton antiporter with K^+ and Na^+ specificity.

Electroneutrality of Vc-NhaP1

To probe whether Vc-NhaP1 mediates electrogenic or electroneutral antiport, inside-out membrane vesicles were isolated from TO114 cells transformed with pVc-NhaP1 or pBAD24 and assayed for $\Delta\psi$ in chloride-free, potassium-free buffer. Vesicles were loaded with diethanolamine prior to the addition of Oxonol V in order to maximize the magnitude of the respiration-generated $\Delta\psi$, and again energized by lactate. The subsequent addition of either K^+ (Fig. 5a, upper traces) or Na^+ (Fig. 5a, lower traces) resulted in no detectable depolarization, indicating that the cation/H^+ antiport by Vc-NhaP1 is electroneutral, with one alkali exchanged cation per proton. Addition of the protonophore CCCP (carbonyl cyanide *m*-chlorophenylhydrazone) short-circuited the membrane for H^+ and thus completely dissipated the respiratory $\Delta\psi$ (the last addition in each trace of Fig. 5a). Valinomycin in the presence of potassium may be used instead of CCCP to dissipate $\Delta\psi$ (the last addition in the left trace of Fig. 5b).

It was important to make sure that under the experimental conditions used the sensitivity of the method was sufficient to register *electrogenic* antiport by a partial depolarization resulting from the operation of an antiporter exchanging more than one H^+ per each alkali cation. To this end, inside-out membrane vesicles were also isolated from TO114/pBVA cells expressing the electrogenic Vc-NhaA, which we cloned in *E. coli* and characterized previously (Resch *et al.*, 2010). Upon the addition of Na^+, these vesicles demonstrated very fast and deep depolarization followed by a slower partial repolarization that apparently reflects activation of the respiratory H^+ pumping in response to the Vc-NhaA-mediated ion currents (Fig. 5b, right trace). This behaviour is typical for an electrogenic antiporter such as NhaA and differentiates it from electroneutral Vc-NhaP2 (Resch *et al.*, 2010) and Vc-NhaP1 (Fig. 5a). In another positive control for the experiments with Vc-NhaP1 shown in Fig. 5, an artificial rather than natural electrogenic cation/proton exchanger was used. 'Empty' TO114/pBAD24 vesicles were pre-treated with a high concentration (5.0 μM) of nigericin, an artificial ion exchanger that acts as an electrogenic

antiporter at concentrations exceeding 1.0 μM (Gómez-Puyou & Gómez-Lojero, 1977; Guffanti *et al.*, 1998). The addition of potassium to the nigericin-treated vesicles after energization by lactate caused detectable depolarization (not shown). Taken together, these $\Delta\psi$ measurements strongly suggest that, like Vc-NhaP2 (Resch *et al.*, 2010) and in contrast to Vc-NhaA, Vc-NhaP1 catalyses the electroneutral ion exchange of one K^+ or Na^+ ion per H^+.

DISCUSSION

Cation/proton antiporters are found across all domains of life, typically serving to maintain cytosolic ion and pH homeostasis as well as turgor pressure (Bakker & Mangerich, 1981; Corratgé-Faillie *et al.*, 2010; Csonka, 1989; Nakamura *et al.*, 1984, 1992; Zilberstein *et al.*, 1982). Not surprisingly, there are many examples of antiporters of different kinds that co-exist in the membranes of micro-organisms exposed to dynamic changes of the ionic composition in the environment, of which many have been described in *V. cholerae* (Dzioba-Winogrodzki *et al.*, 2009; Häse *et al.*, 2001; Miller *et al.*, 1984; Vimont & Berche, 2000). Here, we describe biochemical and some physiological properties of an uncharacterized antiporter, Vc-NhaP1, one of the three NhaP paralogues predicted by the genomic screen of *V. cholerae* (see Table 1 and Resch *et al.*, 2010, 2011). This subgroup of *V. cholerae* antiporters is especially interesting because (i) antiporters of the NhaP type in general have diverse cation selectivities, manifested in a variety of physiological functions (Resch *et al.*, 2011), and (ii) as this work and that of Resch *et al.* (2010) shows, these closely related paralogues indeed differ biochemically, thus offering a rare opportunity to identify structural determinants of their cation specificity and to obtain insights into the events in the ion-binding cavity using site-directed mutagenesis prior to crystallographic analysis. We are currently working in this direction.

Our analysis of growth phenotype of the *Vc-nhaP1* deletion mutant revealed that Vc-NhaP1 is essential for growth of *V. cholerae* at low pH under two distinct conditions: when the concentration of external K^+ exceeds 300 mM (Figs 1a and 2); and when the concentration of alkali cations in the medium is minimal (Figs 1a, d and 2). The former feature, i.e. coping with the high potassium load, is common for Vc-NhaP2 (Resch *et al.*, 2010) and Vc-NhaP1 (this work). It suggests that the two antiporters are co-operating to keep the cytoplasmic concentration of K^+ under toxic levels, by using a relatively high ΔpH [normally existing on the membrane of cells growing in acidic media (Padan *et al.*, 1981)] to expel K^+ in an electroneutral manner (see Resch *et al.*, 2010 for extended analysis); elimination of either antiporter by chromosomal deletion leads to a dramatically lowered growth yield at pH 6.0 and $[K^+] > 300$ mM. In both cases, introduction of the corresponding gene *in trans* complemented the mutant phenotype [Figs 1 and 2 and data in Resch *et al.* (2010)].

The second growth phenotype of the *Vc-nhaP1* deletion mutant, a growth defect observed under minimal alkali cation load at pH 6.0, is unique to Vc-NhaP1. Apparently, this phenotype could not be explained by a simple assumption that in the low-cation environment Vc-NhaP1 mediates a $K^+(Na^+)/H^+$ antiport that removes the excess of H^+ from the cytoplasm in exchange for external alkali cations, because in this case electroneutral Vc-NhaP1 would move ions against both thermodynamic driving forces, ΔpH and ΔpK. Operating in the opposite direction, Vc-NhaP1 would mediate externally directed K^+ flux and thus alleviate the hypo-osmotic stress (Csonka, 1989). One may note here that protons that Vc-NhaP1 brings into the cytoplasm in this case would be promptly removed by respiratory chain. However, our attempts to prove the idea of a role of Vc-NhaP1 in osmoprotection were not entirely successful, because external proline did not rescue the *Vc-nhaP1* deletion phenotype, and sucrose improved the growth only partially. Therefore, we also examined a possible involvement of Vc-NhaP1 in pH regulation (see below).

It is of note that deletion of *Vc-nhaP1* produces a dissimilar response to Li^+ as compared to deletion of *Vc-nhaP2* (Resch *et al.*, 2010). While the elimination of functional Vc-NhaP2 renders cells much more *resistant* to external Li^+ due to the prevention of Vc-NhaP2-dependent hetero-ion $Li^+/K^+(Na^+)$ exchange (see Resch *et al.*, 2010), deletion of *Vc-nhaP1* does not affect the lithium resistance of *V. cholerae* cells in any way (Fig. 1g–i), indicating that Vc-NhaP1, in contrast to its NhaP2 paralogue, cannot bind Li^+ at all.

The above phenotypic analysis indicates that (a) Vc-NhaP1 is able to exchange H^+ for K^+ and, probably, Na^+, but not Li^+ ions; (b) in acidic low-cation media, Vc-NhaP1 possibly affects intracellular osmolarity and/or pH; and (c) Vc-NhaP1-dependent ion exchange is most probably electroneutral, so that Vc-NhaP1 can only expel alkali cations when cells have sufficiently high transmembrane ΔpH (cytoplasm more alkaline, as is the case in acidic growth media) and, vice versa, a chemical transmembrane gradient of a substrate cation (ΔpK or ΔpNa) is required to change intracellular pH.

To check these predictions, we first examined the cation selectivity and electrogenicity of Vc-NhaP1 using the experimental model of inside-out TO114 membrane vesicles containing the heterologously expressed antiporter. As expected, Vc-NhaP1 did not exchange Li^+ for H^+ (Fig. 4, triangles), but both K^+ and Na^+ were the substrates of antiport (Fig. 4, squares and circles, respectively). For K^+, Vc-NhaP1 showed a broad pH optimum at 7.5–8.5, while Na^+/H^+ antiport peaked at pH 8.0–8.5 (experimental pH in the model of inside-out vesicles corresponds to the cytoplasmic pH *in vivo*). Unfortunately, modest levels of observed activity (approx. 16 % dequenching with Na^+ and no more than 11 % with K^+) precluded accurate assessment of affinities of Vc-NhaP1 for its substrate cations. At present, it is not entirely clear why the activity of Vc-NhaP1 is considerably lower than that of Vc-NhaP2 when expressed and assayed under exactly the same conditions [Vc-NhaP2 showed 50 % dequenching at pH 8.0 with K^+ (Resch *et al.*,

2010)], but preliminary immunodetection probes with the V5-tagged variants of Vc-NhaP1 and Vc-NhaP2 indicate that this is due to the intrinsic properties of Vc-NhaP1 rather than problems with its expression and/or targeting (C. Resch, unpublished observations). As Fig. 5(a) shows, neither K^+/H^+ nor Na^+/H^+ antiport via Vc-NhaP1 disturbs $\Delta\psi$ on the vesicular membrane, indicating the electroneutral character of both processes. This also is in accord with the observed phenotype of O395N1Δ*nhaP1*, which is evident under acidic but not neutral or alkaline growth conditions, i.e. only where the ΔpH on the membrane (more acidic outside) is of considerable magnitude (Padan *et al.*, 1981).

Further, we assessed whether Vc-NhaP1 contributes to the control of cytoplasmic pH in acidic external medium. Data presented in Fig. 3 suggest that (i) K^+ rather than Na^+ ions are necessary for the pH homeostasis in *V. cholerae* at external pH 6.0 and (ii) functional Vc-NhaP1 contributes to both efficiency of internal pH recovery (Fig. 3a) and the resulting steady-state level of internal pH (Fig. 3c). It is important to note that the regulation of internal pH in these experiments showed a clear dependence on K^+ supplied externally (Fig. 3a) or internally (Fig. 3c) in a Vc-NhaP1-dependent manner, and not when Na^+ was supplied either externally (Fig. 3b) or internally (Fig. 3c). The capacity of Vc-NhaP1-mediated Na^+ export (Fig. 4) is indeed greater than the antiporter's capacity for K^+ export. However, Vc-NhaP1 is only a small part of the complex Na^+ export machinery of *V. cholerae*, which contains NQR, NhaB and a number of additional Na^+/H^+ antiporters, some of which are expected to be active under our experimental conditions. So, elimination of Vc-NhaP1 in its capacity as Na^+/H^+ antiporter is unlikely to change any sodium-dependent homeostatic mechanism. In contrast, as the data presented in our communication seem to suggest, Vc-NhaP1, when mediating K^+ exchange, contributes to the regulation of internal pH in *V. cholerae*. All these observations support the idea that, at acidic external pH and moderate concentrations of external K^+, Vc-NhaP1 somehow attenuates the cytoplasmic pH by mediating flux of K^+. Elimination of functional Vc-NhaP1 apparently disturbs the homeostasis of cytoplasmic pH under acidic conditions. It is of note that O395N1Δ*nhaP1* retained some capacity for K^+-dependent regulation of cytoplasmic pH (Fig. 3a, c), implying that other components of K^+ homeostasis in *V. cholerae*, namely Vc-NhaP2 and Vc-NhaP3, may partially compensate for the loss of Vc-NhaP1. Further studies will be required to determine the precise contributions of each NhaP paralogue to the regulation of cytoplasmic pH in *V. cholerae*. Curiously, data in Fig. 3, especially Fig. 3(c), clearly suggest that the K^+ transport mediated by Vc-NhaP1 helps to *alkalinize* the cytoplasm of *V. cholerae*. At present, one can only speculate about the molecular mechanism underlying this effect: indeed, as discussed above, electroneutral Vc-NhaP1 in low-ionic acidic media should rather let external protons into the cell in exchange for abundant internal K^+. While our data clearly show a dependence of internal pH regulation on presence of Vc-NhaP1, export of protons into acidic media is thermodynamically unfavourable; therefore, Vc-NhaP1 is necessary for internal pH regulation in *V. cholerae*, but it either has other as-yet undiscovered pleiotropic functions or, more likely, it cooperates with other transporters or antiporters in a manner which at present remains obscure. To resolve this paradox, extensive studies will be required, including the construction and analysis of double and triple mutants with deletions of *nhaP* paralogues, possibly in conjunction with the elimination of selected H^+ and Na^+ pumps.

Cytoplasmic pH is normally tightly regulated over a wide range of extracellular cation concentrations in many bacteria. Cells of *E. coli* maintain a cytosolic pH of 7.4–7.8 when grown in media ranging from pH 5.6 to pH 8.5 (Slonczewski *et al.*, 1981), similar to cells of *V. alginolyticus*, which maintain a cytosolic pH of 7.6–7.8 in media ranging from pH 6.0 to pH 9.0 (Nakamura *et al.*, 1992). Na^+/H^+ antiport has been linked to cytosolic pH homeostasis in *E. coli* at alkaline extracellular pH (Zilberstein *et al.*, 1982). Studies in *E. coli* (Bakker & Mangerich, 1981; Kroll & Booth, 1981, 1983; Slonczewski *et al.*, 1981; Zilberstein *et al.*, 1982) and *V. alginolyticus* (Hamaide *et al.*, 1983; Nakamura *et al.*, 1984, 1992; Tokuda & Unemoto, 1981; Tokuda *et al.*, 1981) showed that K^+ is necessary for regulating cytosolic pH under acidic external conditions. As shown in Table 1, *V. alginolyticus*, like *V. cholerae*, has three *nhaP* paralogues. Data presented in this communication suggest that Vc-NhaP1 could play a role in moderating cytosolic pH when external pH is low. Loss of Vc-NhaP1 resulted in somewhat reduced capacity to control cytosolic pH as well as hypersensitivity to high $[K^+]$ in an acidic environment. It is possible that the primary functions of NhaP-type ion exchangers in *Vibrio* spp. are pH attenuation and protection against K^+ in acidic media.

During growth-curve experiments, a slight biphasic growth was observed in O395N1Δ*nhaP1*/pVc*nhaP1* and O395N1/pBAD24 cells exposed to 500 mM K^+, but not in the uncomplemented mutant (Fig. 2f). Our previous work has shown the importance of Vc-NhaP2 under these conditions (Resch *et al.*, 2010), so it appears that these two paralogues augment each other at high K^+ concentrations. Therefore, this biphasic growth might have been caused by a regulated change in the expression levels of NhaP2 and/or NhaP3 in response to high (approx. 0.5 M) extracellular K^+ concentrations. However, our preliminary measurements of *nhaP* paralogue transcripts in O395N1 by qRT-PCR as a function of $[K^+]$ or $[Na^+]$ at pH 6.0 show no correlation between paralogue expression and $[K^+]$ or $[Na^+]$ (data not shown). As loss of NhaP1 caused no growth inhibition by any of the cations tested at pH 7.2 and higher, as compared to the parent, expression of NhaP1 was not measured under these conditions. The physiological relevance of NhaP paralogues in *V. cholerae* is intriguing, as such high levels of K^+ are not expected to be encountered normally; environmentally, *V. cholerae* is presumably exposed to approximately 7 mM KCl in seawater (Webb, 1939) and the intestine (Watten *et al.*,

1959). It is conceivable, however, that a battery of three NhaP paralogues expelling K^+ might be critical for *V. cholerae* passing the acidic and K^+-rich gastric barrier.

ACKNOWLEDGEMENTS

The authors would like to thank Dr Yusuke Minato for helpful discussions, and Dr Joan L. Slonczewski for the kind gift of pMMB1311. This research was supported by grants from the National Institutes of Health (no. AI-063121-02) and the Natural Sciences and Engineering Research Council of Canada (no. 227414-04).

REFERENCES

Bakker, E. P. & Mangerich, W. E. (1981). Interconversion of components of the bacterial proton motive force by electrogenic potassium transport. *J Bacteriol* **147**, 820–826.

Corratgé-Faillie, C., Jabnoune, M., Zimmermann, S., Véry, A. A., Fizames, C. & Sentenac, H. (2010). Potassium and sodium transport in non-animal cells: the Trk/Ktr/HKT transporter family. *Cell Mol Life Sci* **67**, 2511–2532.

Csonka, L. N. (1989). Physiological and genetic responses of bacteria to osmotic stress. *Microbiol Rev* **53**, 121–147.

Dzioba, J., Ostroumov, E., Winogrodzki, A. & Dibrov, P. (2002). Cloning, functional expression in *Escherichia coli* and primary characterization of a new Na^+/H^+ antiporter, NhaD, of *Vibrio cholerae*. *Mol Cell Biochem* **229**, 119–124.

Dzioba-Winogrodzki, J., Winogrodzki, O., Krulwich, T. A., Boin, M. A., Häse, C. C. & Dibrov, P. (2009). The *Vibrio cholerae* Mrp system: cation/proton antiport properties and enhancement of bile salt resistance in a heterologous host. *J Mol Microbiol Biotechnol* **16**, 176–186.

Enserink, M. (2010). Public health. No vaccines in the time of cholera. *Science* **329**, 1462–1463.

Epstein, W. & Kim, B. S. (1971). Potassium transport loci in *Escherichia coli* K-12. *J Bacteriol* **108**, 639–644.

Gómez-Puyou, A. & Gómez-Lojero, C. (1977). The use of ionophores and channel formers in the study of the function of biological membranes. In *Current Topics in Bioenergetics*, vol. 6, pp. 221–257. Edited by D. Rao Sanadi. New York: Academic Press.

Guffanti, A. A., Cheng, J. & Krulwich, T. A. (1998). Electrogenic antiport activities of the Gram-positive Tet proteins include a $Na^+(K^+)/K^+$ mode that mediates net K^+ uptake. *J Biol Chem* **273**, 26447–26454.

Hamaide, F., Kushner, D. J. & Sprott, G. D. (1983). Proton motive force and Na^+/H^+ antiport in a moderate halophile. *J Bacteriol* **156**, 537–544.

Hamashima, H., Iwasaki, M. & Arai, T. (1995). A simple and rapid method for transformation of *Vibrio* species by electroporation. *Methods Mol Biol* **47**, 155–160.

Häse, C. C., Fedorova, N. D., Galperin, M. Y. & Dibrov, P. A. (2001). Sodium ion cycle in bacterial pathogens: evidence from cross-genome comparisons. *Microbiol Mol Biol Rev* **65**, 353–370.

Ho, S. N., Hunt, H. D., Horton, R. M., Pullen, J. K. & Pease, L. R. (1989). Site-directed mutagenesis by overlap extension using the polymerase chain reaction. *Gene* **77**, 51–59.

Kitko, R. D., Cleeton, R. L., Armentrout, E. I., Lee, G. E., Noguchi, K., Berkmen, M. B., Jones, B. D. & Slonczewski, J. L. (2009). Cytoplasmic acidification and the benzoate transcriptome in *Bacillus subtilis*. *PLoS ONE* **4**, e8255.

Kitko, R. D., Wilks, J. C., Garduque, G. M. & Slonczewski, J. L. (2010). Osmolytes contribute to pH homeostasis of *Escherichia coli*. *PLoS ONE* **5**, e10078.

Kroll, R. G. & Booth, I. R. (1981). The role of potassium transport in the generation of a pH gradient in *Escherichia coli*. *Biochem J* **198**, 691–698.

Kroll, R. G. & Booth, I. R. (1983). The relationship between intracellular pH, the pH gradient and potassium transport in *Escherichia coli*. *Biochem J* **216**, 709–716.

Mekalanos, J. J., Swartz, D. J., Pearson, G. D., Harford, N., Groyne, F. & de Wilde, M. (1983). Cholera toxin genes: nucleotide sequence, deletion analysis and vaccine development. *Nature* **306**, 551–557.

Metcalf, W. W., Jiang, W., Daniels, L. L., Kim, S. K., Haldimann, A. & Wanner, B. L. (1996). Conditionally replicative and conjugative plasmids carrying *lacZα* for cloning, mutagenesis, and allele replacement in bacteria. *Plasmid* **35**, 1–13.

Miller, C. J., Drasar, B. S. & Feachem, R. G. (1984). Response of toxigenic *Vibrio cholerae* O1 to physico-chemical stresses in aquatic environments. *J Hyg (Lond)* **93**, 475–495.

Nakamura, T., Tokuda, H. & Unemoto, T. (1982). Effects of pH and monovalent cations on the potassium ion exit from the marine bacterium, *Vibrio alginolyticus*, and the manipulation of cellular cation contents. *Biomembranes* **692**, 389–396.

Nakamura, T., Tokuda, H. & Unemoto, T. (1984). K^+/H^+ antiporter functions as a regulator of cytoplasmic pH in a marine bacterium, *Vibrio alginolyticus*. *Biochim Biophys Acta* **776**, 330–336.

Nakamura, T., Kawasaki, S. & Unemoto, T. (1992). Roles of K^+ and Na^+ in pH homeostasis and growth of the marine bacterium *Vibrio alginolyticus*. *J Gen Microbiol* **138**, 1271–1276.

Padan, E., Zilberstein, D. & Schuldiner, S. (1981). pH homeostasis in bacteria. *Biochim Biophys Acta* **650**, 151–166.

Padan, E., Maisler, N., Taglicht, D., Karpel, R. & Schuldiner, S. (1989). Deletion of ant in *Escherichia coli* reveals its function in adaptation to high salinity and an alternative Na^+/H^+ antiporter system(s). *J Biol Chem* **264**, 20297–20302.

Radchenko, M. V., Waditee, R., Oshimi, S., Fukuhara, M., Takabe, T. & Nakamura, T. (2006). Cloning, functional expression and primary characterization of *Vibrio parahaemolyticus* K^+/H^+ antiporter genes in *Escherichia coli*. *Mol Microbiol* **59**, 651–663.

Resch, C. T., Winogrodzki, J. L., Patterson, C. T., Lind, E. J., Quinn, M. J., Dibrov, P. & Häse, C. C. (2010). The putative Na^+/H^+ antiporter of *Vibrio cholerae*, Vc-NhaP2, mediates the specific K^+/H^+ exchange in vivo. *Biochemistry* **49**, 2520–2528.

Resch, C. T., Winogrodzki, J. L., Häse, C. C. & Dibrov, P. (2011). Insights into the biochemistry of the ubiquitous NhaP family of cation/H^+ antiporters. *Biochem Cell Biol* **89**, 130–137.

Singleton, F. L., Attwell, R., Jangi, S. & Colwell, R. R. (1982a). Effects of temperature and salinity on *Vibrio cholerae* growth. *Appl Environ Microbiol* **44**, 1047–1058.

Singleton, F. L., Attwell, R. W., Jangi, M. S. & Colwell, R. R. (1982b). Influence of salinity and organic nutrient concentration on survival and growth of *Vibrio cholerae* in aquatic microcosms. *Appl Environ Microbiol* **43**, 1080–1085.

Slonczewski, J. L., Rosen, B. P., Alger, J. R. & Macnab, R. M. (1981). pH homeostasis in *Escherichia coli*: measurement by ^{31}P nuclear magnetic resonance of methylphosphonate and phosphate. *Proc Natl Acad Sci U S A* **78**, 6271–6275.

Tokuda, H. & Unemoto, T. (1981). A respiration-dependent primary sodium extrusion system functioning at alkaline pH in the marine bacterium *Vibrio alginolyticus*. *Biochem Biophys Res Commun* **102**, 265–271.

Tokuda, H. & Unemoto, T. (1982). Characterization of the respiration-dependent Na^+ pump in the marine bacterium *Vibrio alginolyticus*. *J Biol Chem* **257**, 10007–10014.

Tokuda, H., Nakamura, T. & Unemoto, T. (1981). Potassium ion is required for the generation of pH-dependent membrane potential and delta pH by the marine bacterium *Vibrio alginolyticus*. *Biochemistry* **20**, 4198–4203.

Vimont, S. & Berche, P. (2000). NhaA, an Na^+/H^+ antiporter involved in environmental survival of *Vibrio cholerae*. *J Bacteriol* **182**, 2937–2944.

Watten, R. H., Morgan, F. M., Songkhla, Y. N., Vanikiati, B. & Phillips, R. A. (1959). Water and electrolyte studies in cholera. *J Clin Invest* **38**, 1879–1889.

Webb, D. (1939). The sodium and potassium content of seawater. *J Exp Biol* **16**, 178–183.

Zhou, W., Bertsova, Y. V., Feng, B., Tsatsos, P., Verkhovskaya, M. L., Gennis, R. B., Bogachev, A. V. & Barquera, B. (1999). Sequencing and preliminary characterization of the Na^+-translocating NADH: ubiquinone oxidoreductase from *Vibrio harveyi*. *Biochemistry* **38**, 16246–16252.

Zilberstein, D., Agmon, V., Schuldiner, S. & Padan, E. (1982). The sodium/proton antiporter is part of the pH homeostasis mechanism in *Escherichia coli*. *J Biol Chem* **257**, 3687–3691.

Edited by: A. R. Walmsley